melt fraction will be more gradual, reflecting the gradual increase of water solubility in olivine and orthopyroxene.

Our results therefore support the concept that the low-velocity zone may be related to partial melting (*1*, *2*, *6*). However, even in the absence of melting, the partitioning of water between olivine and orthopyroxene would strongly depend on depth. The high water solubilities in aluminous orthopyroxene at low pressure and temperature will effectively "dry out" olivine, and this may also contribute to a stiffening of the lithosphere. In any case, however, our results imply that the existence of an asthenosphere—and therefore of plate tectonics as we know it—is possible only in a planet with a water-bearing mantle.

References and Notes
1. D. L. Anderson, *Theory of the Earth* (Blackwell Scientific, Boston, 1989).
2. D. L. Anderson, C. Sammis, *Phys. Earth Planet. Inter.* **3**, 41 (1970).
3. I. Kushiro, Y. Syono, S. Akimoto, *J. Geophys. Res.* **73**, 6023 (1968).
4. T. Kawamoto, J. R. Holloway, *Science* **276**, 240 (1997).
5. I. B. Lambert, P. J. Wyllie, *Nature* **219**, 1240 (1968).
6. I. B. Lambert, P. J. Wyllie, *Science* **169**, 764 (1970).
7. D. L. Kohlstedt, H. Keppler, D. C. Rubie, *Contrib. Mineral. Petrol.* **123**, 345 (1996).
8. M. Rauch, H. Keppler, *Contrib. Mineral. Petrol.* **143**, 525 (2002).
9. K. Mierdel, H. Keppler, *Contrib. Mineral. Petrol.* **148**, 305 (2004).
10. S.-I. Karato, H. Jung, *Earth Planet. Sci. Lett.* **157**, 193 (1998).
11. G. Hirth, D. L. Kohlstedt, *Earth Planet. Sci. Lett.* **144**, 93 (1996).
12. Y.-H. Zhao, S. B. Ginsberg, D. L. Kohlstedt, *Contrib. Mineral. Petrol.* **147**, 155 (2004).
13. D. R. Bell, P. D. Ihinger, G. R. Rossman, *Am. Mineral.* **80**, 465 (1995).
14. P. A. Danckwerth, R. C. Newton, *Contrib. Mineral. Petrol.* **66**, 189 (1978).
15. D. Perkins, T. J. B. Holland, R. C. Newton, *Contrib. Mineral. Petrol.* **78**, 99 (1981).
16. T. Gasparik, *Phase Diagrams for Geoscientists: An Atlas of the Earth's Interior* (Springer-Verlag, Berlin, 2003).
17. M. Cameron, J. J. Papike, *Rev. Mineral.* **7**, 5 (1980).
18. K. S. Pitzer, S. M. Sterner, *J. Chem. Phys.* **101**, 3111 (1994).
19. R. Lu, H. Keppler, *Contrib. Mineral. Petrol.* **129**, 35 (1997).
20. R. Stalder, H. Skogby, *Eur. J. Mineral.* **14**, 1139 (2002).
21. See supporting material on *Science* Online.
22. D. R. Bell, G. R. Rossman, *Science* **255**, 1391 (1992).
23. J. Ingrin, H. Skogby, *Eur. J. Mineral.* **12**, 543 (2000).
24. N. Bolfan-Casanova, *Mineral. Mag.* **69**, 229 (2005).
25. C. A. Rychert, K. M. Fischer, S. Rondenay, *Nature* **436**, 542 (2005).
26. D. L. Turcotte, G. Schubert, *Geodynamics* (Cambridge Univ. Press, Cambridge, ed. 2, 2002).
27. D. R. Bell, G. R. Rossman, J. Maldener, D. Endisch, F. Rauch, *J. Geophys. Res.* **108**, 10.1029/2001JB000679 (2003).
28. M. S. Paterson, *Bull. Mineral.* **105**, 20 (1982).
29. Supported by a Deutsche Forschungsgemeinschaft Leibniz award (H.K.) and by the Alexander von Humboldt Foundation and NSF grant EAR 0337611 (J.R.S.).

A Semi-Empirical Approach to Projecting Future Sea-Level Rise

Stefan Rahmstorf

A semi-empirical relation is presented that connects global sea-level rise to global mean surface temperature. It is proposed that, for time scales relevant to anthropogenic warming, the rate of sea-level rise is roughly proportional to the magnitude of warming above the temperatures of the pre–Industrial Age. This holds to good approximation for temperature and sea-level changes during the 20th century, with a proportionality constant of 3.4 millimeters/year per °C. When applied to future warming scenarios of the Intergovernmental Panel on Climate Change, this relationship results in a projected sea-level rise in 2100 of 0.5 to 1.4 meters above the 1990 level.

Understanding global sea-level changes is a difficult physical problem, because complex mechanisms with different time scales play a role (*1*), including thermal expansion of water due to the uptake and penetration of heat into the oceans, input of water into the ocean from glaciers and ice sheets, and changed water storage on land. Ice sheets have the largest potential effect, because their complete melting would result in a global sea-level rise of about 70 m. Yet their dynamics are poorly understood, and the key processes that control the response of ice flow to a warming climate are not included in current ice sheet models [for example, meltwater lubrication of the ice sheet bed (*2*) or increased ice stream flow after the removal of buttressing ice shelves (*3*)]. Large uncertainties exist even in the projection of thermal expansion, and estimates of the total volume of ice in mountain glaciers and ice caps that are remote from the continental ice sheets are uncertain by a factor of two (*4*). Finally, there are as yet no published physically based projections of ice loss from glaciers and ice caps fringing Greenland and Antarctica.

For this reason, our capability for calculating future sea-level changes in response to a given surface warming scenario with present physics-based models is very limited, and models are not able to fully reproduce the sea-level rise of recent decades. Rates of sea-level rise calculated with climate and ice sheet models are generally lower than observed rates. Since 1990, observed sea level has followed the uppermost uncertainty limit of the Intergovernmental Panel on Climate Change (IPCC) Third Assessment Report (TAR), which was constructed by assuming the highest emission scenario combined with the highest climate sensitivity and adding an ad hoc amount of sea-level rise for "ice sheet uncertainty" (*1*).

While process-based physical models of sea-level rise are not yet mature, semi-empirical models can provide a pragmatic alternative to estimate the sea-level response. This is also the approach taken for predicting tides along coasts (for example, the well-known tide tables), where the driver (tidal forces) is known, but the calcula-tion of the sea-level response from first principles is so complex that semi-empirical relationships perform better. Likewise, with current and future sea-level rise, the driver is known [global warming (*1*)], but the computation of the link between the driver and the response from first principles remains elusive. Here, we will explore a semi-empirical method for estimating sea-level rise.

As a driver, we will use the global average near-surface air temperature, which is the standard diagnostic used to describe global warming. Figure 1 shows a schematic response to a step-function increase in temperature, after climate and sea level parameters were at equilibrium. We expect sea level to rise as the ocean takes up heat and ice starts to melt, until (asymptotically) a new equilibrium sea level is reached. Paleoclimatic data suggest that changes in the final equilibrium level may be very large: Sea level at the Last Glacial Maximum, about 20,000 years ago, was 120 m lower than the current level, whereas global mean temperature was 4° to 7°C lower (*5*, *6*). Three million years ago, during the Pliocene, the average climate was about 2° to 3°C warmer and sea level was
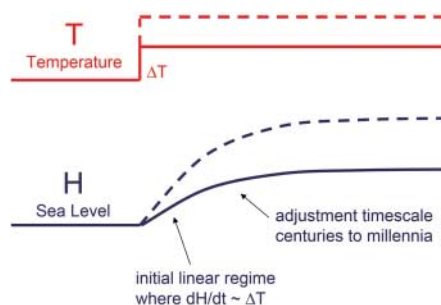

Fig. 1. Schematic of the response of sea level to a temperature change. The solid line and the dashed line indicate two examples with different amplitude of temperature change.

Potsdam Institute for Climate Impact Research, 14473 Potsdam, Germany. E-mail: rahmstorf@ozean-klima.de

25 to 35 m higher (7) than today's values. These data suggest changes in sea level on the order of 10 to 30 m per °C.

The initial rate of rise is expected to be proportional to the temperature increase

$$dH/dt = a\,(T - T_0) \qquad (1)$$

where H is the global mean sea level, t is time, a is the proportionality constant, T is the global mean temperature, and T_0 is the previous equilibrium temperature value. The equilibration time scale is expected to be on the order of millennia. Even if the exact shape of the time evolution $H(t)$ is not known, we can approximate it by assuming a linear increase in the early phase; the long time scales of the relevant processes give us hope that this linear approximation may be valid for a few centuries. As long as this approximation holds, the sea-level rise above the previous equilibrium state can be computed as

$$H(t) = a\int_{t0}^{t}(T(t') - T_0)\,dt' \qquad (2)$$

where t' is the time variable.

We test this relationship with observed data sets of global sea level (8) and temperature [combined land and ocean temperatures obtained from NASA (9)] for the period 1880–2001, which is the time of overlap for both series. A highly significant correlation of global temperature and the rate of sea-level rise is found ($r = 0.88$, $P = 1.6 \times 10^{-8}$) (Fig. 2) with a slope of $a = 3.4$ mm/year per °C. If we divide the magnitude of equilibrium sea-level changes that are suggested by paleoclimatic data (5–7) by this rate of rise, we obtain a time scale of 3000 to 9000 years, which supports the long equilibration time scale of sea-level changes.

The baseline temperature T_0, at which sea-level rise is zero, is 0.5°C below the mean temperature of the period 1951–1980. This result is consistent with proxy estimates of temperatures in the centuries preceding the modern warming (10), confirming that temperature and sea level were not far from equilibrium before this modern warming began. This is consistent with the time scale estimated above and the relatively stable climate of the Holocene (the past 10,000 years).

In Fig. 3, we compare the time evolution of global mean temperature, converted to a "hindcast" rate of sea-level rise according to Eq. 1, with the observed rate of sea-level rise. This comparison shows a close correspondence of the two rates over the 20th century. Like global temperature evolution, the rate of sea-level rise increases in two major phases: before 1940 and again after about 1980. It is this figure that most clearly demonstrates the validity of Eq. 1. Accordingly, the sea level that was computed by integrating global temperature with the use of Eq. 2 is in excellent agreement with the observed sea level (Fig. 3), with differences always well below 1 cm.

We can explore the consequences of this semi-empirical relationship for future sea levels (Fig. 4), using the range of 21st century temperature scenarios of the IPCC (1) as input into Eq. 2. These scenarios, which span a range of temperature increase from 1.4° to 5.8°C between 1990 and 2100, lead to a best estimate of sea-level rise of 55 to 125 cm over this period. By including the statistical error of the fit shown in Fig. 2 (one SD),

the range is extended from 50 to 140 cm. These numbers are significantly higher than the model-based estimates of the IPCC for the same set of temperature scenarios, which gave a range from 21 to 70 cm (or from 9 to 88 cm, if the ad hoc term for ice sheet uncertainty is included). These semi-empirical scenarios smoothly join with the observed trend in 1990 and are in good agreement with it during the period of overlap.

We checked that this analysis is robust within a wide range of embedding periods (i.e., smoothing) of the observational time series. The slope found in Fig. 2 varies between 3.2 and 3.5 mm/year per °C for any embedding period between 2 and 17 years, causing only minor variations in the projected sea level. For short embedding periods (around 5 years), the rate of sea-level rise (Fig. 3, top) closely resembles that shown in (8) with large short-term fluctuations. For embedding dimensions longer than 17 years, the slope starts to decline, because the acceleration of sea-level rise since 1980 (Fig. 3) is then progressively lost by excessive smoothing. For very long embedding periods (30 years), the rate of sea-level rise becomes rather flat such as that shown in (11).

The linear approximation (Eq. 1) is only a simplistic first-order approximation to a number of complex processes with different time scales. The statistical error included in Fig. 4 does not include any systematic error that arises if the linear relationship breaks down during the forecast period. We can test for this systematic error using climate models, if only for the thermal expansion component of sea-level rise that these models capture. For this test, we used the CLIMBER-3α climate model (12), which uses a simplified atmosphere model coupled to a three-dimensional general circulation ocean model with free surface (i.e., that vertically adjusts). We used a model experiment initialized from an equilibrium state of the coupled system in the year 1750 and, with historic radiative forcing, forced changes until the year 2000. After 2000, the model was forced with the IPCC A1FI scenario. The global mean temperature increases by 0.8°C in the 20th century and by 5.0°C from 1990 to 2100 in this experiment.

Temperature and sea-level rise data from this model for the time period 1880–2000 were treated like the observational data in the analysis presented above, and graphs corresponding to Figs. 2 and 3 look similar to those derived from the observational data (figs. S1 and S2). The slope found is only 1.6 mm/year per °C (i.e., half of the observed slope) because only the thermal expansion component is modeled. Using the semi-empirical relation as fitted to the period 1880–2000, we predicted the sea level for the 21st century (fig. S3). Up to the year 2075, this predicted sea level remains within 5 cm of the actual (modeled) sea level. By the year 2100, the predicted level is 51 cm whereas the actual (modeled) level is 39 cm above that of 1990 (i.e., the semi-empirical formula overpredicts sea level by 12 cm).

For the continental ice component of sea-level rise, we do not have good models to test how the

Fig. 3. (**Top**) Rate of sea-level rise obtained from tide gauge observations (red line, smoothed as described in the Fig. 2 legend) and computed from global mean temperature from Eq. 1 (dark blue line). The light blue band indicates the statistical error (one SD) of the simple linear prediction (15). (**Bottom**) Sea level relative to 1990 obtained from observations (red line, smoothed as described in the Fig. 2 legend) and computed from global mean temperature from Eq. 2 (blue line). The red squares mark the unsmoothed, annual sea-level data.
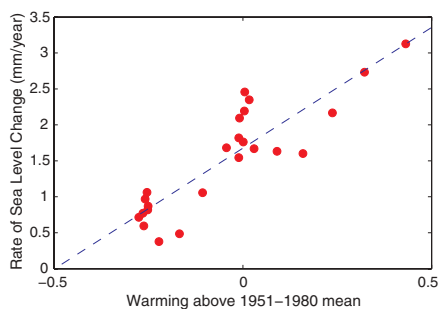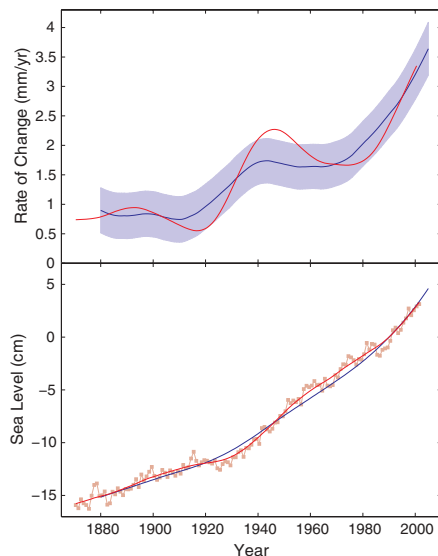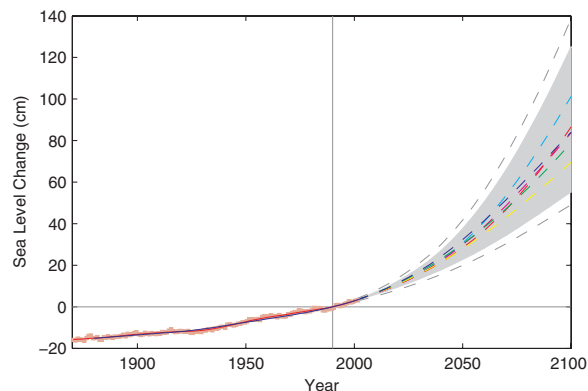
Fig. 2. Correlation of temperature and the rate of sea-level rise for the period 1881–2001. The dashed line indicates the linear fit. Both temperature and sea-level curves were smoothed by computing nonlinear trend lines, with an embedding period of 15 years (14). The rate of sea-level change is the time derivative of this smoothed sea-level curve, which is shown in Fig. 3. Data were binned in 5-year averages to illustrate this correlation.

Fig. 4. Past sea level and sea-level projections from 1990 to 2100 based on global mean temperature projections of the IPCC TAR. The gray uncertainty range spans the range of temperature rise of 1.4° to 5.8° C, having been combined with the best statistical fit shown in Fig. 2. The dashed gray lines show the added uncertainty due to the statistical error of the fit of Fig. 2. Colored dashed lines are the individual scenarios as shown in (1); the light blue line is the A1FI scenario, and the yellow line is the B1 scenario.

linear approximation performs, although the approximation is frequently used by glaciologists ("degree-days scheme"). Given the dynamical response of ice sheets observed in recent decades and their growing contribution to overall sea-level rise, this approximation may not be robust. The ice sheets may respond more strongly to temperature in the 21st century than would be suggested by a linear fit to the 20th century data, if time-lagged positive feedbacks come into play (for example, bed lubrication, loss of buttressing ice shelves, and ocean warming at the grounding line of ice streams). On the other hand, many small mountain glaciers may disappear within this century and cease to contribute to sea-level rise. It is therefore difficult to say whether the linear assumption overall leads to an over- or underestimation of future sea level. Occam's razor suggests that it is prudent to accept the linear assumption as reasonable, although it should be kept in mind that a large uncertainty exists, which is not fully captured in the range shown in Fig. 4.

Regarding the lowest plausible limit to sea-level rise, a possible assumption may be that the rate shown in Fig. 3 stops increasing within a few years (although it is difficult to see a physical reason for this) and settles at a constant value of 3.5 mm/year. This implies a sea-level rise of 38 cm from 1990 to 2100. Any lower value would require that the rate of sea-level rise drops despite rising temperature, reversing the relationship found in Fig. 2.

Although a full physical understanding of sea-level rise is lacking, the uncertainty in future sea-level rise is probably larger than previously estimated. A rise of over 1 m by 2100 for strong warming scenarios cannot be ruled out, because all that such a rise would require is that the linear relation of the rate of sea-level rise and temperature, which was found to be valid in the 20th century, remains valid in the 21st century. On the other hand, very low sea-level rise values as reported in the IPCC TAR now appear rather implausible in the light of the observational data.

The possibility of a faster sea-level rise needs to be considered when planning adaptation measures, such as coastal defenses, or mitigation measures designed to keep future sea-level rise within certain limits [for example, the 1-m long-term limit proposed by the German Advisory Council on Global Change (13)].

References and Notes

1. J. T. Houghton et al., Eds., *Climate Change 2001: The Scientific Basis* (Cambridge Univ. Press, Cambridge, 2001).
2. H. J. Zwally et al., *Science* **297**, 218 (2002).
3. E. Rignot et al., *Geophys. Res. Lett.* **31**, 18 (2004).
4. S. C. B. Raper, R. J. Braithwaite, *Nature* **439**, 311 (2006).
5. C. Waelbroeck et al., *Quat. Sci. Rev.* **21**, 295 (2002).
6. T. Schneider von Deimling, A. Ganopolski, H. Held, S. Rahmstorf, *Geophys. Res. Lett.* **33**, L14709 (2006).
7. H. J. Dowsett et al., *Global Planet. Change* **9**, 169 (1994).
8. J. A. Church, N. J. White, *Geophys. Res. Lett.* **33**, L01602 (2006).
9. J. Hansen et al., *J. Geophys. Res. Atmos.* **106**, 23947 (2001).
10. P. D. Jones, M. E. Mann, *Rev. Geophys.* **42**, RG2002 (2004).
11. S. Jevrejeva, A. Grinsted, J. C. Moore, S. Holgate, *J. Geophys. Res.* **111**, 09012 (2006).
12. M. Montoya et al., *Clim. Dyn.* **25**, 237 (2005).
13. German Advisory Council on Global Change, "The future oceans: warming up, rising high, turning sour," (Wissenschaftlicher Beirat der Bundesregierung Globale Umweltveränderungen Special Report, Berlin, 2006); (www.wbgu.de/wbgu_sn2006_en.pdf).
14. J. C. Moore, A. Grinsted, S. Jevrejeva, *Eos* **86**, 226 (2005).
15. The statistical error was calculated by means of the Matlab function "polyval" for the linear fit shown in Fig. 2.
16. The author thanks J. Church for providing the observational data and M. Stöckmann for the model data. They as well as J. Gregory and B. Hare are thanked for valuable discussions.

Nonequilibrium Mechanics of Active Cytoskeletal Networks

Daisuke Mizuno,[1] Catherine Tardin,[1] C. F. Schmidt,[1,2]* F. C. MacKintosh[1]*

Cells both actively generate and sensitively react to forces through their mechanical framework, the cytoskeleton, which is a nonequilibrium composite material including polymers and motor proteins. We measured the dynamics and mechanical properties of a simple three-component model system consisting of myosin II, actin filaments, and cross-linkers. In this system, stresses arising from motor activity controlled the cytoskeletal network mechanics, increasing stiffness by a factor of nearly 100 and qualitatively changing the viscoelastic response of the network in an adenosine triphosphate–dependent manner. We present a quantitative theoretical model connecting the large-scale properties of this active gel to molecular force generation.

Mechanics directly control many functions of cells, including the generation of forces, motion, and the sensing of external forces (1). The cytoskeleton is a network of semiflexible linear protein polymers (actin filaments, microtubules, and intermediate filaments) that is responsible for most of the mechanical functions of cells. It differs from common polymer materials in both the complexity of composition and the fact that the system is not at thermodynamic equilibrium. Chemical nonequilibrium drives mechanoenzymes (motor proteins) that are the force generators in cells. The cytoskeleton is thus an active material that can adapt its mechanics and perform mechanical tasks such as cell locomotion or cell division.

Here, we show how nonequilibrium motor activity controls the mechanical properties of a simple three-component in vitro model cytoskeletal network. The nonequilibrium origin of this active control mechanism can be seen directly in the violation of a fundamental theorem of statistical physics, the fluctuation-dissipation (FD) theorem, which links thermal fluctuations of systems to their response to external forces. The FD theorem is a generalization of Einstein's description of Brownian motion (2). Although it is valid only in equilibrium, its possible extension to out-of-equilibrium systems such as granular materials and living cells has been debated (3–5). Prior studies in cells have suggested violations of the FD theorem (3), but this has not been directly observed. We show that an in vitro model system consisting of a cross-linked

[1]Department of Physics and Astronomy, Vrije Universiteit, 1081HV Amsterdam, Netherlands. [2]III. Physikalisches Institut, Fakultät für Physik, Georg-August-Universität, 37077 Göttingen, Germany.

*To whom correspondence should be addressed. E-mail: cfs@nat.vu.nl (C.F.S.); fcm@nat.vu.nl (F.C.M.)